Editorial Manager(tm) for Environmental Fluid Mechanics
Manuscript Draft

Manuscript Number: EFMC219R2

Title: Dynamics of the Buoyant plume off the Pearl River Estuary in summer

Article Type: Original Research

Keywords: Pearl River Estuary; buoyant plume; the northern shelf of SCS; river discharge; wind

Corresponding Author: Dr Hong Zhang,

Corresponding Author's Institution: Griffith University

First Author: Suying Oh

Order of Authors: Suying Oh; Hong Zhang; Dong-xiao Wang

Abstract: Field measurements of salinity, wind and river discharge and numerical simulations of hydrodynamics from 1978 to 1984 are used to investigate the dynamics of the buoyant plume off the Pearl River Estuary (PRE), China during summer. The studies have shown that there are four major horizontal buoyant plume types in summer: Offshore Bulge Spreading (Type I), West Alongshore Spreading (Type II), East Offshore Spreading (Type III), and Symmetrical Alongshore Spreading (Type IV). River mouth conditions, winds and ambient coastal currents have inter-influences to the transport processes of the buoyant plume. It is found that all of the four types are surface-advected plumes by analysing the vertical characteristic of the plumes, and the monthly variations of the river discharge affect the plume size dominantly. The correlation coefficient between the PRE plume size and the river discharge reaches 0.85 during the high river discharge season. A wind strength index has been introduced to examine the wind effect. It is confirmed that winds play a significant role in forming the plume morphology. The alongshore wind stress and the coastal currents determine the alongshore plume spreading. The impact of the ambient currents such as Dongsha Current and South China Sea (SCS) Warm Current on the plume off the shelf has also assessed. The present study has demonstrated that both the river discharge and wind conditions affect the plume evolution.

Response to Reviewers: See the attached letter for the respond to reviewers.

Dynamics of the Buoyant plume off the Pearl River Estuary in summer

Suying Ou[†‡], Hong Zhang[∞*], Dong-xiao Wang[§]

[†] Institute of Oceanology, Chinese Academy of Sciences, Qingdao 266071, China
[∞]Griffith School of Engineering, Griffith University, QLD 4217, Australia
[‡] Institute of Estuarine and Coastal Research, Zhong-Shan University, Guangzhou 510275, China.
[§]South China Sea Institute of Oceanology, Chinese Academy of Sciences, Guangzhou 510301, China

Abstract

Field measurements of salinity, wind and river discharge and numerical simulations of hydrodynamics from 1978 to 1984 are used to investigate the dynamics of the buoyant plume off the Pearl River Estuary (PRE), China during summer. The studies have shown that there are four major horizontal buoyant plume types in summer: Offshore Bulge Spreading (Type I), West Alongshore Spreading (Type II), East Offshore Spreading (Type III), and Symmetrical Alongshore Spreading (Type IV). River mouth conditions, winds and ambient coastal currents have inter-influences to the transport processes of the buoyant plume. It is found that all of the four types are surface-advected plumes by analysing the vertical characteristic of the plumes, and the monthly variations of the river discharge affect the plume size dominantly. The correlation coefficient between the PRE plume size and the river discharge reaches 0.85 during the high river discharge season. A wind strength index has been introduced to examine the wind effect. It is confirmed that winds play a significant role in forming the plume morphology. The alongshore wind stress and the coastal currents determine the alongshore plume spreading. The impact of the ambient currents such as Dongsha Current and South China Sea (SCS) Warm Current on the plume off the shelf has also assessed. The present study has demonstrated that both the river discharge and wind conditions affect the plume evolution.

Key wards: Pearl River Estuary; buoyant plume; the northern shelf of SCS; river discharge; wind

*Corresponding author: hong.zhang@griffith.edu.au

1 Introduction

Continental shelves associated with large river systems typically receive a large amount of freshwater and sediment discharge which can influence coastal circulations, coastal sediment budgets and other chemical/biological transport processes. The mechanism of freshwater discharged into the continental shelf has been studied intensively. Many of these large river estuarine and shelf buoyant plumes, such as the Amazon, the Changjiang and the Mississippi, have received the most attentions due to their large discharge amount to the ocean. A series of previous studies have been conducted based on the field monitoring data and numerical simulations to understand a variety of plume structures inside and outside the estuary (*Lentz*, 1995*; Lentz and Limeburner*, 1995*; Walker*, 1996*; Estourneal*, 1997*; Zhu et al.*, 1997*; Geyer*, 2000). It was found that the dynamic processes of the buoyant plume were controlled by various oceanic dynamic forces, river mouth conditions and the topography of the adjacent ocean. *Pu* (2002) confirmed the south spreading of Changjiang plume and the northeast spreading which is dominated by the summer monsoon wind, the cold eddy and the current of Yellow Sea. Two Rhone plumes responding against wind conditions had also been documented by *Estourneal* (1997). The detailed plume morphology of Mississippi Plume was analysed using satellite data by *Walker* (1996). *Yankovsky and Chapman* (1997) developed criteria to categorize two types of plumes based on the bottom topography information.

In the last two decades, various techniques including field measurements, satellite observations and numerical models have been adopted to understand the buoyant plume structures and their associated circulations under different forcing. *Chao and Boicourt* (1986) and *Chao* (1988) are the earliest to apply an ocean model with idealized topography to examine the effects of wind and river discharge on buoyancy plumes. *Gavine* (1995) introduced scaling analysis to assess the contribution of advection terms and Coriolis force to the buoyant plume, which are important for interpreting observations and model results. The dependence of three-dimensional plume characteristics on model parameters were investigated (*Kourafalou and Lee*, 1996; *Garvine*, 1999; *Kourafalou*, 1999; *Garvine* 2001). A conceptual model was developed to study the impact of an upwelling wind to the surface-advected plume by *Fong and Geyer* (2001). Their model simulations demonstrate that the plume thins and is advected offshore by the cross-shore Ekman transport. The advection of cross-shore salinity gradients and vertical mixing controls the evolution of the plum.

More recently, the bulge shape of the plume has been studied (*Fong and Geyer*, 2002), which appears to be a prominent characteristic. With neglecting the wind effect, the ocean current has been showed to be the significant factor to the bulge shaping. This is further confirmed by laboratory experiments by *Horner-Devine et al.* (2006). However, the wind influence on a coastal buoyant plume was

investigated using a wind strength index by *Whitney and Garvine* (2005). It found that the across-shelf plume is more sensitive to wind influence than the along shore flow. A bi-directional plume in Columbia river was presented by *Hickey et al.* (2005). The influence of the wind and the ambient current was studied. Therefore, it is of great significance to have a comprehensive understanding of the plume shaping in relationship with the river mouth condition, the wind and the ambient current.

The Pearl River ranks as the 13th largest river in the world with an annual runoff of 3.36×10^{11} m^3 to the Pearl River Estuary (PRE). Since 1950s, fundamental research on its hydrographic features in the PRE had been conducted, particularly the tide driven mixing process between salt water and fresh water. More recently, some studies have been carried out to examine the buoyant plume during summer. *Ma et al.* (1990) pointed out the low-salinity water of PRE spread eastwards due to southwest monsoon, and spreads westerly affected by other factors during summer. *Xue et al.* (2001) studied the mechanism of Pearl River plume based on numerical simulations and suggested that the spreading path of low-salinity water of Pearl River depends on winds, inshore surface heights and runoffs. Recently, the PRE plume in winter and its estuary circulation were also studied numerically (*Wong et al.*, 2004). The seasonal variation of the Pearl River Plume was described, and the physical processes in the PRE were studied empirically (Dong et al., 2004). The mechanism of biological or biogeochemical processes and sediment transport process near the PRE, and the influences of the PRE plume on its processes were also explored (*Yin et al.* 2004; *Cai et al.*, 2004; *Ying*, 1999). However, the study focus is within the PRE region, while the plume characteristics outside the estuarine have only been pre-analysed by *Ou et al.* (2007) recently. The morphology of the buoyant plume in summer (June - August) was explored with the inter-decadal monthly field data from 1978 to 1984.

In early studies in others regions, few researchers have accesses to synoptic measurements such as this from 1978-1984 over 7 years (*Ma et al.*, 1990). The data would allow us to investigate the summer characteristics of buoyant plume in ways that few other plume studies have been able to. In particular, only a few researchers have considered the complexity in plume shaping that results form wind conditions. Therefore, in the present study, the comprehensive long time monitoring data and a numerical model are to be applied to study the buoyant plume dynamics and to assess the impacts of the river discharge, the wind and the ambient current on the PRE plume.

2 Monitoring data review

The Pearl River Estuary (PRE) is located in between of the Taiwan Shoal and the Hainan Island of the northern South China Sea (SCS). In the present study, the PRE and its adjacent continental shelf with

an ENE–WSW orientation covering about *(150, 300) km* in both direction were included, which is shown in Figure 1.

From 1978 to 1984, a continuous hydrologic survey in the northern SCS was carried out and the details of the survey can be obtained in *Ma et al.* (1990). The measured transects and stations are marked in Figure 1. The survey was conducted monthly from 1978 to 1981 and bimonthly from 1982 to 1984. The measured parameters included the water depth, the salinity, the temperature, the wind, the PH value and the wave height. The collected comprehensive datasets not only provide information for the ocean resources exploitation, the ocean engineering, the navigation and the ocean environment assessment, but also for a further study on coastal dynamics.

The Pearl River's drainage basin is located entirely in a subtropical zone and dominated by monsoonal climate, which determines the winds and the Pearl River runoffs. The northeastern monsoon prevails in winter and the Pearl River discharge is smallest. When the southwestern monsoon begins in April–May, the flood season also begins. Usually, the southwestern monsoon prevails in summer and becomes strongest in July with the annual peak discharge of the Pearl River .The spring is the transitional seasons from the northern monsoon to southwestern monsoon while the autumn reverses. The dominant wind of every month in the study area during 1978 to 1984 is shown in Table 1. In the study region, the local southwest, the south, the southeast and the east winds occur most frequently in the region during summer monsoon. Figure 2 shows the Pearl River discharge during 1978 to 1984. The seasonal discharge variation of the Pearl River is significant. In the flood season between April-September, the Pearl River receives the 78% of the annual runoff. In summer (June - August), 50% of the runoff runs into the northern of SCS through the Pear River, while only 10% runoff flows into PRE estuary in winter (December – February). It is known that in summer the northern continental shelf of SCS off PRE is greatly influenced by the large amount of freshwater discharged from the Pearl River. The low salinity water spreads off PRE and floats on the continental shelf which is driven by complex oceanic forces, i.e. a buoyant plume typically forms in summer. However, *Dong et al.* (2004) studied the PRE plume in July of 1999 and 2000, and January of 2000. It was found that the plume only appeared within the PRE in the winter of 2000. Therefore, it is important to have further study on the plume in the study area, as the data collected by *Dong et al.* (2004) in the PRE region lacks of full spatial distribution of salinity on the northern shelf of SCS.

In last two decades, only a few scattered monitoring datasets were collected on the northern shelf of SCS. The data collected by South China Sea Branch from 1978 to 1984 is still the most comprehensive to investigate the horizontal seaward limit and variations of PRE buoyant plume during large river discharge season.

3 Buoyant plume characteristics

3.1 Horizontal characteristics

In order to emphasize both the plume spreading direction and offshore bulge, the study area is partitioned into three regions as shown in Figure 3: PRE region, Western Guangdong Sea region (WGS) and Eastern Guangdong Sea region (EGS). The salinity isohaline of 32 *psu* is determined to be the offshore boundary of the buoyant plume.

In early studies, *Chao* (1988) used the non-dimensional parameter λ_r, which is the ratio between the offshore bulge width and the width of the coastal current to characterise plumes. The plume is determined to be a bulge shape (supercritical) if $\lambda_r > 1.7$, or be alongshore spreading (subcritical) if $\lambda_r < 1.7$. *Kourafalou and Lee* (1996) also found that the value of λ_r is close to 1 in their numerical simulation results with high eddy viscosity diffusive plume. Under most circumstances, the alongshore spreading plume behaviour prevails under the strong mixing due to tides and winds. In the present study, the non-dimensional parameters representing the discharge conditions and the scale of the buoyant plume have been derived to classify the plume structure. They are:

$$\lambda = \frac{L}{L_c} \text{ and } \lambda_I = \frac{L_E}{L_w}, \quad (1)$$

where L is defined as the maximum spreading distance between the boundary salinity isohaline (i.e *S=32 psu*) and the river mouth in the PRE region; L_E refers to the maximum spreading distance from PRE boundary to the boundary salinity isohaline in EGS region; L_W is defined as the maximum spreading extent from PRE boundary to the boundary salinity isohaline in the WGS region; and L_C is defined as the seaward plume width at the boundary between the PRE and the WGS region. The parameter specifications are illustrated in Figure 3.

The monitoring data collected in summers from 1978 to 1984 are analysed. The plume shapes in terms of L, L_c, L_E and L_W are analysed using simple statistics techniques and listed in Table 2. The buoyant plumes off PRE can be classified into four types using the parameters such as λ and λ_I - Offshore Bulge Spreading (Type I), West Alongshore Spreading (Type II), East Offshore Spreading (Type III) and Symmetrical Alongshore Spreading (Type IV), and the details are summarized as follows.

Type I - Offshore Bulge Spreading

Offshore Bulge Spreading is a typical freshwater plume. When the large amount of low-salinity water extends seaward strongly or the alongshore current is weak, the buoyant discharge turns right in the northern hemisphere under Corilis force. The westward (L_W) and eastward spreading (L_E) of the plume are relatively small. Figure 4(a) shows the examples of Type I plume. The low-salinity water is

confined to the nearshore zone of WGS with L_W of *56 km*. The eastward spreading L_E only reaches *31 km* where is close to Hong Kong sea. However, the offshore extension, L, is about *116 km*. The plume structure shows that the extent of offshore spreading L is much larger than L_W and L_E. In an agreement with *Chao* (1988) and *Kourafalou and Lee* (1996)'s research, it has $\lambda >$ 1.7 and $\lambda_1 <$1. It can be found in Table 2 that there are two Type I plumes existed in July 1980 and August 1984 during the experiment period.

Type II - West Alongshore Spreading

If the plume extended progressively westward with the restricted eastward spreading, i.e. $L_W > L_E$; and the offshore intrusion, L, is small comparing to L_W, i.e. $\lambda <$1.7 and $\lambda_1 <$1, the plume with is defined as Type II plume - West Alongshore Spreading. In the summers from 1978 to 1984, the Type II is one of the most common structures especially in June as summarised in Table 2. Figure 4 (b) shows one of the examples in June 1979. It can be seen that the buoyant plumes is typical westwardly extended, where the low-salinity water was carried from the mouth of PRE to the western region of Hainan Island, but the eastward extension was stopped near Hong Kong coast. A larger portion of freshwater flows offshore and westwardly, as shown in Figure 4 (b). The bulge shape changes with time, the farthest of which can flow up to the Hainan Island ($L_W > 240km$), while the nearest one only bypassing the YangJiang ($L_W \approx 130km$). The plume type is clearly subcritical as $\lambda < 1.7$. It might be due to the increased land ward friction force, the strengthened horizontal and vertical eddy diffusion or downwelling favorable winds.

Type III - East Offshore Spreading

The dominant characteristic of the Type III - East Offshore Spreading plume is that the low-salinity water from PRE flows offshore and eastwardly to EGS, but not alongshore eastwardly, as shown in Figure 4(c). The plume boundary at the continental shelf breaks near Dongsha Islands with $L_O >$0. This is the most distinctive characteristic which is totally different from other plumes. Type III plume is typically subcritical with $\lambda <$1.7, and L_W may reach a large value, but L_E is even larger than L_W, i.e. $\lambda_1 >$1. The low-salinity water moves offshore near DaYa Bay towards the eastern continental shelf rather than alongshore towards Shantou nearshore region, where the upwelling current along the EGS coast occurs often.

Type IV - Symmetrical Alongshore Spreading

Type IV buoyant plume always evolves from the Type III plume. For Type III plumes, the criteria for the nondimentional parameters still the same as that of Type II plumes, i.e. λ_1>1 and λ<1.7, but there is no plume boundary breaking at the continental shelf. For these plumes, the low salinity water occupied both westward and eastward alongshore regions with limited spreading in the offshore direction as a symmetrical distribution as in Figure 4(d). When the Type IV plume forms, the EGS upwelling current always disappears along the coast. Figure 4(d) also shows that the salinity increases from the coast to the open sea and the low salinity water is more coastally trapped comparing to Type III plume as in Figure 4(c). This characteristic is another difference between Type III and IV plumes.

3.2 Vertical characteristic

Figure 5 shows the typical vertical profiles of the salinity along various transects at *113°E, 114°E* and *115°E*. But it is necessary to point out that due to the limited availability of measured data (the vertical profiling distance is between *5-10 m*), some contour lines are attracted together. The figure shows that the water is clearly stratified that the low-salinity water floats on top of the high salinity water near PRE. As the low-salinity water in Pearl River Estuary flows offshore, the high-salinity continental shelf water compensates as upwelling current along seabed towards inner continental shelf or invades into the estuary directly. For all plumes, the thickness of buoyant plume is small comparing to the water depth. The thickness in the PRE ranges between *5-15 m*. From the river mouth to the lateral nearshore region, the buoyant plume advects and mixes gradually with shelf water, where the thickness of buoyant plume decreases and diminishes eventually. All the plumes of PRE haven't reached the sea bottom.

The plumes as shown in Figure 5 are defined as the surface-advected plumes by *Yankovsky and Chapman* (1997). The trapping depth of the plume, h_b, and the horizontal length scaling parameter, L_s, are applied to predict the behaviour of the plume based on its dynamic characteristics. The equations signifying h_b and L_s can be written as (*Horner-Devine et al.*, 2006)

$$h_b = \left(\frac{2Qf}{g'} \right)^{1/2}, \tag{2}$$

$$L_s = \frac{6g'h_0 + 2V_i^2}{f\left(2g'h_0 + V_i^2\right)^{\frac{1}{2}}}, \tag{3}$$

where Q is the river discharge rate; V_i is the velocity of buoyant inflow as it enters the shelf; h_0 is the average depth of the mouth; and the reduced gravity g' is given by $g' = \rho' g / \rho_0$, where ρ' is the density difference.

In the PRE, $h_0 = 10$ *m*, and the mean velocity V_i of fresh water into the shelf ranged *0.3~0.4 m/s* under different discharge in summer as shown in Figure 2. The computed trapping depth h_b ranges *4.0-5.0 m* with $h_b < h_0$. Therefore the bottom boundary layer has no significant influence on the buoyant plume transport. The PRE plume can be classified as surface-advected, and the predicted L_s ranges *40-112 km*, which is in consistence with the observed L_C as in Table 2.

4 Dynamics of buoyant plumes

Studies in other large rivers such as the ChangJiang and the Mississippi have confirmed that the variation of the plume size and the behaviour of the buoyant plume off the PRE are influenced by the river discharge, the bathymetry, the Coriolis force, tides, winds and other mixing processes. These driven forces are also dominant for the evolution of PRE buoyant plumes in summer. The details of their impacts to the buoyant plume are included as follows.

4.1 Influence of river discharge and Coriolis force

A quantitative investigation of the spatial and temporal variability of the Mississippi sediment plume size was conducted by *Walker* (1996). It has been identified the river discharge is one of the most important environmental forcing affecting the plume size, and the Mississippi plume size and the river discharge were well correlated. This relationship has been also confirmed by analysing the PRE data as shown in Figures 6 and 7. Figures 6(a)-(b) indicate the variation of the plume size and the river discharge in June and August from 1978 to 1984. It is found that the plume size depends on the river discharge. For example, the maximal plume size in August 1979 is *50,000* km^2, which occurs with the largest river discharge of *22,000* m^3/s. A high correlated coefficient, *0.85*, indicates that the plume size increase typically with the river discharge increasing. The peak river discharge of one year indicate a large buoyant plume size, but the lag of the low-salinity water transport causes the abnormal large plume size compared to the relative small monthly river discharge. For example, as shown in Table 2, the huge Pearl river discharge of May and June, 1978 (both *~23,000* m^3/s), cause the plume size of July, 1978 reach *61550* km^2, although the monthly averaged river discharge of July is only *11604* m^3/s. In August, 1978, the residual effect of the earlier large discharge decreased abruptly, and the area of low-salinity water is *18070* km^2, only 33% that of July, regardless the river discharges in these two months.

The correlated index between the summer averaged discharge and the summer-averaged plume size from 1978 to 1984 comes to *0.92*, for the residual effect of the earlier large discharge decreased. Figure 7 shows that the comparison of the river discharge and plume size from the monitoring data and from the empirical formula $P \approx \alpha Q^{\beta/0.85}$ (*Warrick and Fong*, 2004), where the location-based

parameters $\alpha = 400$ and $\beta = 0.3$. It can be seen that they are in a good agreement. Consequently, the monthly variation of Pearl River discharge leads to the monthly variation of the average plume size. For the strongest summer monsoon always come with strong river discharge, the largest river discharge in summer to the shelf always formed Type III plume.

In the model study, the buoyant discharge turns anticyclonicly under Coriolis force predominantly toward the down-shelf direction at its source in the Northern Hemisphere without wind, tide and other forces (*Garvine*, 2001). An offshore bulge plume as Type I is formed off the mouth of the estuary, which is due to the large density driven current. A Coriolis force driven anti-cyclonical circulation can be formed on the upper layer near the mouth (*Chao*, 1988; *Kourafalou and Lee*, 1996). The Coriolis effect does result in a lateral asymmetry in both salinity distribution and the circulation driven by the river discharge and the density difference. Numerical simulations have shown that an ideal offshore bulge of plume would be disappeared or change into another form if the force condition changes (*Kourafalou and Lee*, 1996).

4.2 The influence of winds

Early studies have shown that the plume shaping is highly correlated to wind conditions (*Walker*, 1996; *Estourneal*, 1997; *Yin et al.*, 2004; *Hickey et al*, 2005). The surface current system in the SCS is largely dominated by the South Asian Monsoon. The winds blowing down-shelf or up-shelf are denoted as downwelling favorable winds or upwelling favorable winds respectively in the region. Downwelling favorable winds supplement the down-shelf flow and compress the plume towards the coast, while upwelling favorable winds oppose the buoyant plume and spread it offshore. The statistical data of wind observations from 1978 to 1984 are shown in Table 1. It can be seen that during June to August, the dominant winds include E, SE winds, which are downwelling winds, and SW winds which are upwelling winds. Therefore, during summer monsoon periods, the varied northern continental winds would introduce different surface currents and affect the spreading of the PRE plume consequently.

The vertical profiles of plumes in Figure 5 have shown that the PRE plumes in summer are surface-advected, and the bottom friction has little influence to the buoyant plumes. *Whitney and Garvine* (2005) introduced the wind strength index to assess the wind impact to the plume shaping. The wind strength index, I_w is defined as

$$I_w = \frac{u_{wind}}{u_{ds}}, \tag{4}$$

where u_{wind} is the alongshore wind generated current velocity and u_{ds} is the down-shelf buoyancy-

driven velocity. They can be calculated using

$$u_{wind} = \sqrt{\frac{\rho_a}{\rho}\frac{C_{10}}{C_{Da}}}U_{10}$$
$$u_{ds} = \frac{1}{K}\left(2g_r' Qf\right)^{\frac{1}{4}}, \quad with \;\; g_r' = \frac{g(\rho_a - \rho_r)}{\rho_a} \qquad (5)$$

where U_{10} is the wind velocity component at *10 m* height; C_{10} (1.2×10^{-3}) is the surface drag coefficient; C_{Da} (2×10^{-3}) is the depth averaged drag coefficient; ρ_a, ρ and ρ_r are densities of the air , the coastal water and the river water respectively; Q is the river discharge; f is the planetary vorticity; and K is the internal Kelvin number.

I_w defined in equation (4) is the index to compare the wind generated along-shore current and the buoyancy-driven coastal current. When $|I_w|<1$, the river discharge forcing is dominant, i.e. Type I plume would be formed. If taking the down-shelf flow direction as positive, I_w is positive during downwelling favoratble winds and negative during upwelling favorable winds. Therefore, when $|I_w|>1$, the wind contribution is greater than that from the buoyant flow. With consideration of the wind direction, for downwelling favorable winds, i.e $I_w>1$, Type II plume will be formed; for upwelling favorable winds, i.e $I_w<-1$, Tpye III plume will be formed. When $|I_w|\approx1$, the along-shore wind induced current and the buoyancy-driven flow are comparative, Type IV plume should be developed.

The study area with an ENE-WSW orientation lies at the west boundary of the SCS. Considering the alongshore wind component, both the dominant S and SW winds have NE alongshore wind component, while the SE and E winds have SW alongshore wind component. It means that the S and SW winds in the study domain can produce NE coastal current, and the SE and E winds can drive a westward coastal current. However, the statistical wind data of June to August in Table 2 shows the monthly variations of local winds, which may cause the local change of coastal current and have an important role in the monthly change of the plume structure during summer.

The Easterly Guangdong Coastal Current (EGCC) in the northern shelf of SCS is generated by the southwest monsoonal winds as shown in Figure 9. During the wet season, the plume moves towards northeast with prevailing S or SW winds. The northeast extended low salinity water can induce the coastal upwelling at many places along the coast of Guangdong (*Han et al.*, 1988; *Hong et al*., 1991). However, the Westerly Guangdong Coastal Current (WGCC) in WGS region occurs throughout a year (*Huang et al.*, 1992; *Ying*, 1999). The contribution of the WGCC to the plume spreading will be investigated further.

Climatic average COADS winds (*da Silva et al.* 1994) in 1978-1984 are used to depict the plume morphology in high river discharge conditions. I_w from June to August in 1978-1984 is calculated using Equations (4)-(5). The detailed discussion is as follows.

The influence of downwelling-favorable winds (E and SE winds)

Table 3 shows that E or SE winds occur most frequently in June and often in August. The monthly averaged winds generate the westward alongshore current with the range of *1.2-4.8 cm/s*. The wind-driven alongshore current is in the same direction of WGCC. The combined current pushes the river discharge toward the southwest side of the PRE. In EGS region, the wind-current is dominant comparing to the opposite EGCC. The discharged fresh water from the Pearl River moves southward and then turns to the southwest coastal zone following the *50-m* bathymetry isobath approximately. Consequently, the salinity distributions clearly reveal that the plume moves westward as Type II plume shown in Figure 8(A) with I_w=1.79. All Type II plumes in Table 3 confirm the prolonged episodes of strong E or SE winds can cause the extreme spreading of westward plumes in PRE with $I_w > 1$. This is in an agreement with the findings of *Yin et al.* (2004) and *Whitney and Garvine* (2005).

The influence of upwelling-favorable winds (SW wind and S winds)

During the wet season, especially in summer, the upwelling-favorable winds prevail in SCS. Southwest wind events occur most frequently in July as shown in Table 3. The monthly averaged winds generate the eastward alongshore current within the range of *1.3-3.3 cm/s*. The buoyant plume morphology under southwest winds is different from that under E and SE winds. The southwest wind is an upwelling wind. The alongshore component with the EGCC pushes buoyant plume eastward along the shore line. Its cross-shore wind stress component drives the PRE buoyant plume offshore to be separated from the eastward moving plume as shown in Figure 8(B) with I_w=-2.99. The Type III plume demonstrates that strong southwest winds and the EGCC can cause the separation of the PRE River plume from the coast, with a surface plume transport directly to the east. The location of the splitting always appears in the DaYa Bay and Shantou which agrees with early studies (*Han and Ma,* 1988; *Hong and Li,* 1991). The brackish waters from PRE moves southward and curves eastward across the *20-m* to *100-m* isobath closely, and the furthest spreading is off the *200-m* isobath near the DongSha Islands for the prolonged and strong southwest winds and the high river discharge. The plume separating from coast and moving offshore during an upwelling favorable wind have also been demonstrated by *Fong et al.* (2001) using a simple model and three-dimensional model.

The south wind event often occurs on the offshore shelf and the most frequently in the ocean between HaiNan Island and PRE during typical summer monsoon, where the southwest wind prevails on the

other part of SCS at the same time. The monthly averaged south winds would cause a surface transport toward the shore and the estuary, and the alongshore current component is *0.3-2.9 cm/s* for Type IV as shown in Table 3 with $|I_w| \approx 1$. If the upwelling-favorable winds continue several days for half month, Type III plume formed with $I_w < -1$. Then winds change to downwelling-favorable winds, the earlier eastern part of Type III plume move closer to the coast and Type IV plume will be formed though the averaged wind is S wind. The buoyant low-salinity water is trapped in coastal zone, and its offshore movement is constricted. Type IV plume is the bi-directional plume like the Columbia River plume in summer (*Hickey et al*, 2005) under alternative directional winds. Figure 8(C) shows that the east and southwest winds appear alternatively on the shallow sea and the average wind flows southerly. Therefore the plume extends towards southwest and northeast along the coastal zone, and a Type IV buoyant plume is eventually formed. However, when the alongshore current is relative small (*0.5~1.0 cm/s*), a Type I plume might form under the southerly wind with $|I_w| < 1$.

4.3 The influence of other ocean currents

The northern continental shelf of SCS is a micro-tidal region, and the mean tidal range is small with the range of *0.85–1.0 m* outside PRE (*Zhao*, 1990). But inside PRE, the surface elevation and tidal current are influenced by the topography and the river discharge. The tide in the PRE increases gradually with propagating upstream and the mean tidal range reaches *1.7 m* at the upper estuary. The amplitude of the dominant M_2 tide increases from *0.33 m* outside PRE to 0.*65 m* at the upper estuary (*Mao et al*., 2004). The tidal current is one of the dominant current in the northern shelf of SCS, but its net transport is small. Therefore, it has little influence on the spreading direction of the buoyant plume outside PRE, but it enhances the mixing intensity.

The South China Sea Warm Current (SCSWC) and the Dongsha Current (a southwesterly flow passing through Dongsha Islands) also attributed significantly to the hydrodynamics in the study area, as shown in Figure 9. SCSWC flow northeastward throughout the year and it spreads over most parts of the shelf outside the coastal current zone during the summer monsoon (*Huang et al.*, 1992; *Su*, 2004). Combined with the northeastward wind-driven flow, SCSWC enhances the northeastward spreading of the low-salinity water floating on the outer shelf and limits the southerly spreading during high river discharge. It especially affects the formation and evolution of Type III plume.

During summer, Dongsha Current proximity to the Dongsha Islands is a southwesterly flow beneath the surface northeasterly wind drift (*Su*, 2004). The Dongsha Current and the SCSWC locate on the lower continental slope and the outer shelf area, which have little role in the horizontal distribution of the buoyant plume in most conditions discussed. Only under some special conditions such as a very

large river discharge and continued homogenous winds in June and July of 1979, the Dongsha current and SCSWC may influence the plume after leaving the shelf.

5 The evolution of the buoyant plume off PRE

It has been found that the plume area is highly correlated to the monthly Pearl River discharge, and wind conditions determine the buoyant plume type. When the winds and the river discharge have strong seasonal characteristics, the buoyant plumes have typical seasonal variation as well. For example, the seasonal characteristics of the PRE plume in 1979 are presented in Figure 10.

In the summer, the large quantity of fresh water which occupied *51%* of the annual runoff pours into PRE and spreads outward on the top of sea waters. The buoyant plume forms and spreads eastward up to Shantou and westward up to the Hainan Island in July, 1979, as in Figures 10(d).

In winter, only *6%* of the annual runoff entered into PRE, the salt water can intrude in the estuary for the rapid reduced river dynamic (Figure 10(h)). With long mixing time and mixing distance, the water is well mixed, the winter PRE plumes are solely confined within the estuary with a plume size less than *2000* km^2.

The spring and the autumn are transitional seasons in inter-monsoon period. There is about *40%* fresh water of the annual runoff flowing into the PRE estuary. After a long dry winter, the monthly averaged Pearl River discharge in April 1979 increased to *8000*m^3/s, which is still less than the annual averaged river discharge *10130* m^3/s. The low-salinity water stays near the estuary, as shown in Figure 10(a). The river discharge in October 1979 is only *5800* m^3/s, but a Type II plume is formed under the northeast and east winds. This is due to the pre-existing plume produced by the very large monthly averaged discharge (*22000* m^3/s) in September 1979, as shown in Figure 10(f, g).

In the summer period of June to August, the PRE buoyant plume varies. Four types of PRE buoyant plume have been revealed as discussed in Sections 3 and 4. It was more likely to form Type II plume in June. In July, the river discharge is the largest and the dominant wind changes to the upwelling wind, the extension of low-salinity water has a great chance to be Type III plume. However, in August, the plume spreading direction varies, which depends on the contribution from different forcing. All four types of spreading pattern can be found as shown in Table 2.

The effects of the river discharge, wind and other forces on PRE buoyant plume in summer are summarized in Figure 10. When the flood season starts in April, the result plume is still in estuary and there is no buoyant plume on the shelf. With the Pearl River discharge increasing, the Type II buoyant plume begins to form in May under an averaged east wind. Usually, the river discharge in June is very

large and the dominant wind is still downwelling-favorable wind, then Type II plume is formed. In July, the summer monsoon is the strongest and the prevailing winds changes to the upwelling winds. At the same time, the Pearl River discharge is largest and the extensive low-salinity water forms the Type III plume where the main axis of freshwater turns eastward. But if the river discharge in June and July are not large enough, the eastern spreading distance, L_E, of low-salinity water is short under the upwelling winds, and the structure of plume is more like a Type I plume (e.g. in July, 1980). If the upwelling wind in July continues to prevail in August, Type III plume will be formed. But if the dominant winds change inversely to the down-welling wind, Type III plume first evolved to Type IV plume, and then changes to the Type II plume with a long lasting down-welling wind. In the long wet season (June to August), the plume size is always large, and the plume types in July and August are all Type III plume under up-welling winds, and then Type IV plume in September under down-welling winds (see Figure 10).

The buoyant plume characteristics in summer also vary. Assuming the plume is completely confined in the PRE estuary in dry season with the size of 2000 km^2. The monthly time series of plume area from 1978 to 1983 are shown in Figure 11 with comparison with the river discharge. It can be seen that the lag between the plume area and the river discharge is small. The plume area depends on the starting time of the wet season, the flood intensity and when the summer monsoon breaks out. In most of the years, the plume size reaches the peak when the river discharge is the largest. If the wet season begins early, such as in 1983 when the wet season begins in March and the largest river discharge occurs in May, Type III plume is formed in May and then Type IV plume exists in June. In 1980, the wet season begins from April as usual, and the river discharge of wet season is less than that in 1979 (see Figure 11), the summer plume size in 1980 is consequently smaller. From June to August, when the monthly averaged discharge increased from *10629* m^3/s to *16606* m^3/s, the winds changes from down-welling winds in June to weak up-welling winds in July and strong up-welling winds in August, the buoyant plume evolves from Type II to Type I, then Type III. Therefore, the buoyant plume size can be estimated using the observation data of the river discharge and the meteorologic winds. The evolution of plume behaviours can also be predicted.

6 Conclusions

The comprehensive field measurements of the salinity, the Pearl River discharge and wind conditions and numerical simulations of the hydrodynamics from 1978 to 1984 are used to investigate the morphology of the buoyant plume off PRE in summer. Both the horizontal and vertical distributions of

the buoyant plume off PRE are analysed. The dynamic influences of the river discharge, winds and other ocean currents on the PRE plume structure are also discussed. They are summarised as:

1. There are four morphology types of the buoyant plume outside PRE during summer. Type I refers to the offshore bulge spreading, where the low-salinity water extended seaward, but the westward and eastward spreading extents of low-salinity water are limited. This type is controlled by Coriolis force and affected by relative weak environmental force. Type II is defined as the westward alongshore spreading, where the low-salinity water of PRE extended progressively westward, while the eastward extension is restricted. Type III points to the eastward offshore spreading, where the low-salinity water is carried offshore and eastward. Type IV refers to the symmetrical western and eastern alongshore spreading, where the low saline water extends towards the east and the west alongshore symmetrically.
2. All the four types of the plume are surface-advected, and have no interactions with the sea bottom.
3. It is revealed that the river discharge is the most important factor to the size and the shape of plumes around the PRE. The monthly river discharge is highly correlated to the plume size. The correlation coefficient reaches 0.85 in summer. The lag between the plume area and the river discharge is small in normal conditions. Generally, in a wet season, a Type II plume is formed initially; then it is evolved to Type III plume under strong summer monsoon and the corresponding strong river discharge. But a Type IV or a Type II plume can be formed under down-welling winds.
4. It is found that winds play a very important role in forming the plume morphology in the northern shelf of SCS in summer. The alongshore wind stress and the coastal currents determine the alongshore plume spreading. During summer monsoon, the southwest, the south, the southeast and the east winds occur most frequently. East and southeast winds drive the buoyant plume westward to form a Type II plume. Strong southwest winds can cause the separation of the eastward plume and move offshore to form a Type III plume. South winds confine the offshore spreading, but drive the PRE plume eastward and westward symmetrically to form a Type IV plume. When the alongshore current is large but with opposing wind, a Type I plume might form.
5. When the plume extends progressively outside the shelf, the plume dynamic would be affected by other circulations of the northern of SCS such as Dongsha Current and SCS Warm Current.

In the present study, a better understanding of the transport dynamics of the buoyant plume is obtained. The governing parameters and plume characteristics for the four types of horizontal buoyant plumes are summarised in Table 4. This is of great significance for the further study of other coastal processes such as the sediment transport t and the physical/biological interactions related to PRE. At present, the

wave effects have not been taken into account. It would be greatly recommended to study the relationship between the tide, the current, the wave with the buoyant plume and the sediment dispersion outside PRE.

Acknowledgement

The authors would like to thank Dr. H.Y. Xia for his valuable comments, and the South China Sea Branch of China for providing measurements data. This research was partially supported by the Chinese Natural Science Fund (40576013), Innovation Fund of Chinese Academy of Sciences (kzcx3-sw-227) and Australia Research Council International Linkage Award (LX0455606).

References

Cai, W. J., Dai, M.H. and Wang, Y.C., 2004. The biogeochemistry of inorganic carbon and nutrients in the Pearl River estuary and the adjacent Northern South China Sea. Continental Shelf Research, 24, 1301–1319.

Chao, S.Y., 1988a. River-forced estuarine plumes. Journal of Physical Oceanography, 18, 72–88.

Chao, S.Y., 1988b. Wind-driven motion of estuarine plumes. Journal of Physical Oceanography, 18, 1144–1166.

Da Silva A.M., Young, C. and Levitus, S., 1994. Atlas of Surface Marine Data 1994, 1: Algorithms and Procedures. NOAA Atlas NESDIS 6[R]. U.S. Gov. Printing Office, Wash., D.C., 83.

Dong, L.X., Su, J.L., Wong, L.A. and Cao, Z.Y., 2004. Seasonal variation and dynamics of The Pearl River plume. Continental Shelf Research, 24, 1761-1777.

Estourneal, C., 1997. The plume of Rhine: numerical simulation and remote sensing. Continental shelf research, 17, 8, 889-924.

Fong, D.A. and Geyer, W.R., 2001. Response of a river plume during an upwelling favorable wind event. Journal of Geophysical Research 106, 1067-1084.

Garvine, R.W., 1999. Penetration of buoyant coastal discharge onto the continental shelf: a numerical model experiment. Journal of Physical Oceanography, 29, 1892-1909.

Garvine, R., 2001. The impact of model configuration in studies of buoyant coastal discharge. Journal of Marine Research 59, 193-225.

Geyer, W.R, 2000. The structure of the Eel River plume during floods. Continental Shelf Research, 20, 2067-2093.

Han, W.Y. and Ma, K.M., 1988. Study on the upwelling current alongshore Eastern GuangDong. Acta oceanography, 10, 1, 52-59 (in Chinese)

Hickey, B., Geier, S., Kachel, N. and MacFadyen, A., 2005. A bi-directional river plume: The

Columbia in summer. Continental Shelf Research 25, 1631-1656.
Hong, Q.M. and Li, L., 1991. The upwelling current on the shelf of Eastern GuangDong. Journal of TaiWan Strait, 10, 3, 271-277 (in Chinese).
Horner-Devine, A.R., Fong, D.A., Monismith, S.G. and Maxworthy, T., 2006. Laboratory experiments simulating a coastal river inflow. Journal of Fluid Mechanics 555:203-232.
Huang, Q. Z., Wang, W.Z and Li, Y.S., 1992. General situations of the current and eddy in the South China Sea. Journal of Progress in Earth Science, 7, 5, 1-9 (in Chinese).
Kourafalou, V.H. and Lee, T.N., 1996a. The fate of river discharge on the continental shelf 1, Modeling the river plume and the inner shelf coastal current. Journal of Geophysical Research, 101(C2), 3415-3434.
Kourafalou, V.H. and Lee, T.N., 1996b. The fate of river discharge on the continental shelf 2, Transport of coastal low-salinity waters under realistic wind and tidal forcing. Journal of Geophysical Research, 101(C2), 3435-3455.
Kourafalou, V.H., 1999. Process studies on the Po River plume, North Adriatic Sea. Journal of Geophysical Research, 104, 29963 – 29985.
Lentz, S.J. and Limeburner, R., 1995. The Amazon River plume during AMASSEDS: spatial characteristics and salinity variability. Journal of Geophysical Research, 100(C2), 2355-2375.
Lentz, S.J., 1995. The Amazons River Plume during AMASSEDS: Subtidal current variability and the importance of wind forcing. Journal of Geophysical Research, 100(C2), 2377-2390.
Luo, X.L., Yang, Q.S. and Luo, Z.R., 2002. Evolution of river bed in Pearl River delta. Zhongshan University Press, Guangzhou, 10-30 (in Chinese).
Ma, Y.L., Xu, S.G. and Zhong, H.L., 1990. Report on ten-year investigation of hydrologic section in continental shelf nearshore region of northern South China Sea. Ocean Press, Beijing, 1-93 (in Chinese).
Mao, Q.W., Shi, P. and Yin, K. D., 2004. Tides and tidal currents in the Pearl River Estuary. Continental Shelf Research, 24, 1797–1808.
Ou, S.Y., Zhang, H. and Wang, D.X., 2007. Horizontal Characteristics of Buoyant Plume off the Pearl River Estuary during summer. Journal of Coastal Research, SI 50, 652 – 657.
Pu, Y.X. ,1983. Study on the spreading mechanism of the Changjiang River low-salinity water. East Sea Science, 1:43-51 (in Chinese).
Su, J.L., 2004. Overview of the South China Sea circulation and its influence on the coastal physical oceanography outside the Pearl River Estuary. Continental Shelf Research, 24, 1745–1760.
Xue, H.J., Cai, F., Xu, D. and Shi, M., 2001. Characteristics and seasonal variation of the coastal current in the South China Sea. Oceanography in China, 13, 64–75 (in Chinese).

Walker, N.D., 1996. Satellite assessment of Mississippi River plume variability: cause and predictability. Remote sensing environment, 58, 21-35.

Warrick, J.A., and Fong, D.A., 2004. Dispersal scaling from the worlds rivers. Geophysical Research Letters 31: doi:10.1029/2003GL019114.

Whitney, M. M. and Garvine, R.W., 2005. Wind influence on a coastal buoyant outflow. Journal of Geophysical Research 110: C03014, doi:10.1029 /2003JC002261.

Wong, L.A., Chen, J.C. and Dong, L.X., 2004. A model of the plume front of the Pearl River Estuary, China and adjaceng coastal waters in the winter dry season. Continental Shelf Research, 24, 1779-1795.

Yankovsky, A.E. and Chapman, D.C., 1997: A simple theory for the fate of buoyant coastal discharges. Journal of Physical Oceanography, 27, 1386-1401.

Ying, Z.P., 1999. Coastal current and sedimentation along the western GuangDong. Journal of ZhongShan University, 38, 3, 85-89 (in Chinese).

Yin, K.D., Zhang, J. and Qian, P. Y., 2004. Effect of wind events on phytoplankton blooms in the Pearl River estuary during summer. Continental Shelf Research, 24, 1909–1923.

Zhao, H.T., 1990. Evolution of Pearl River Estuary. China Ocean Press, Beijing, 116–147 (in Chinese).

Zhu, J.R., Li, Y.P. and Shen, H.T., 1997. Numerical simulation of the wind field's impact on the expansion of the Changjiang River low salinity water in summer. Oceanology and Limnology, 28, 1, 72-79 (in Chinese).

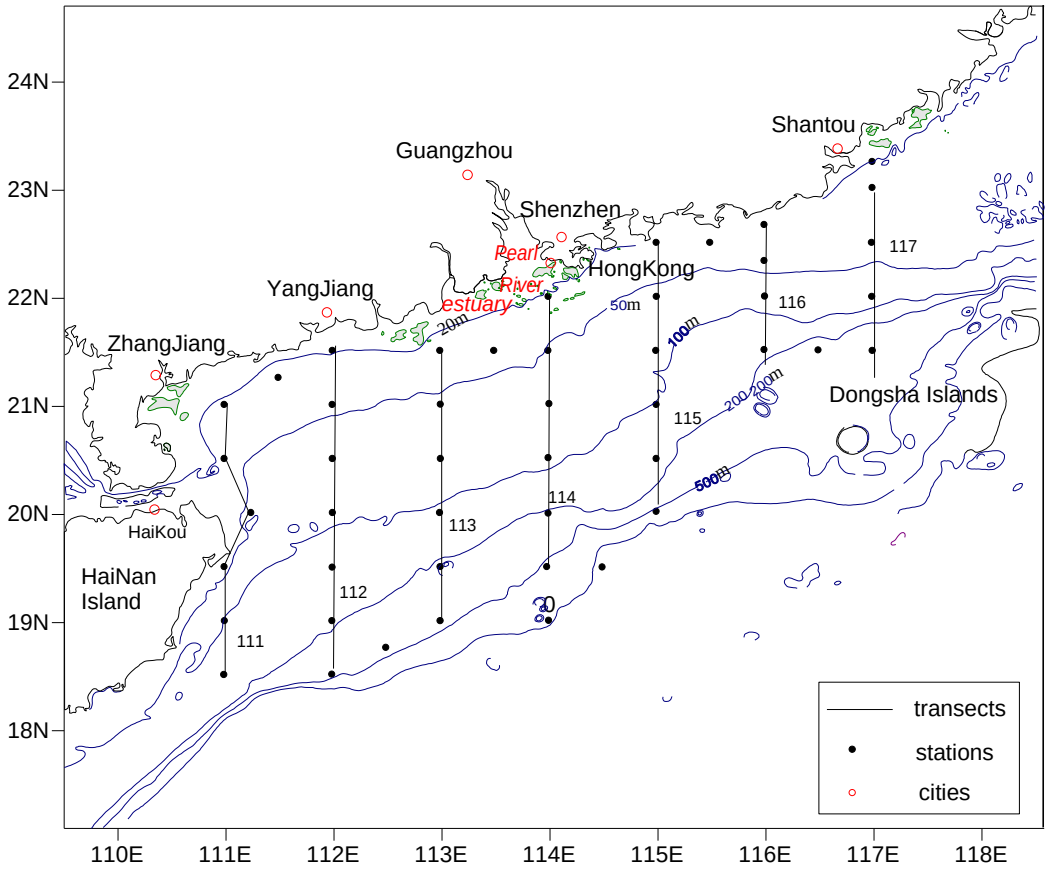

Figure 1: The topography of study area and locations of investigated transects and stations.

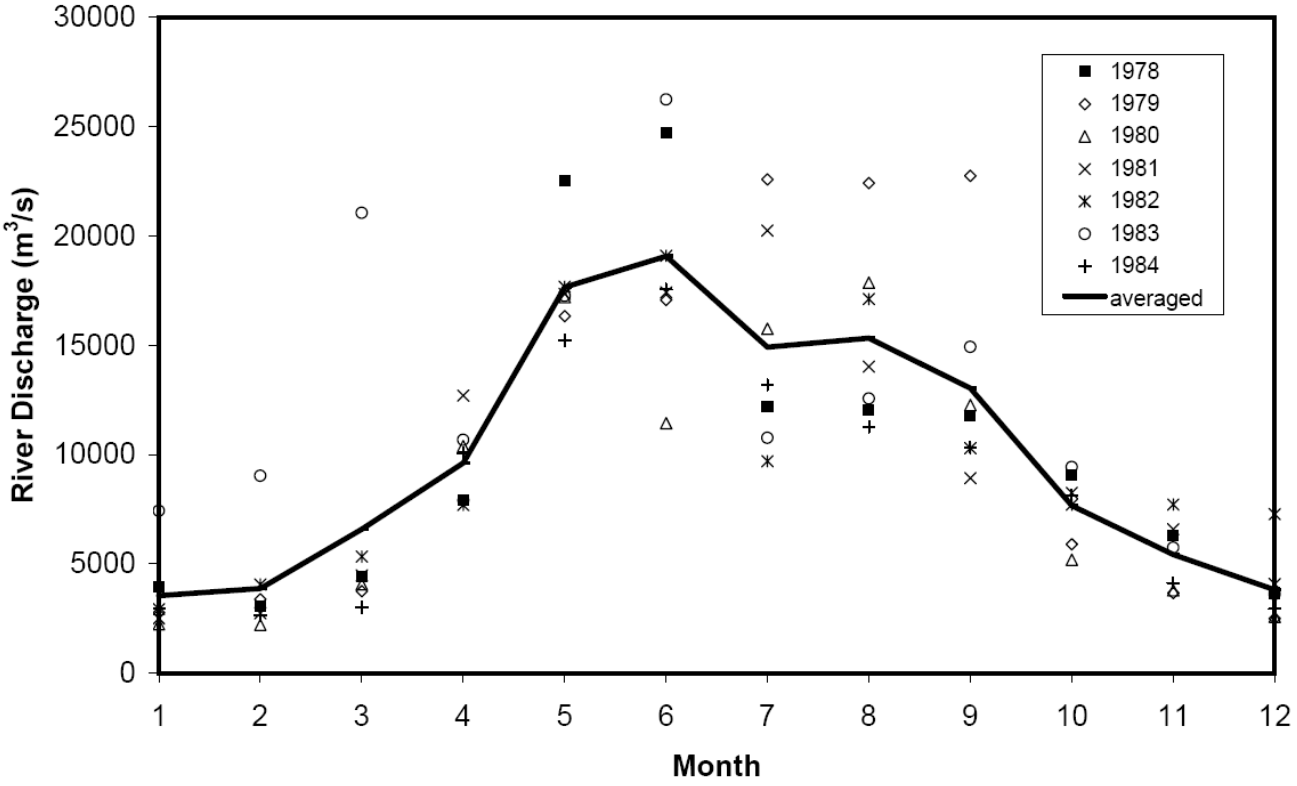

Figure 2: The monthly averaged discharge of Pearl River during 1978 to 1984.

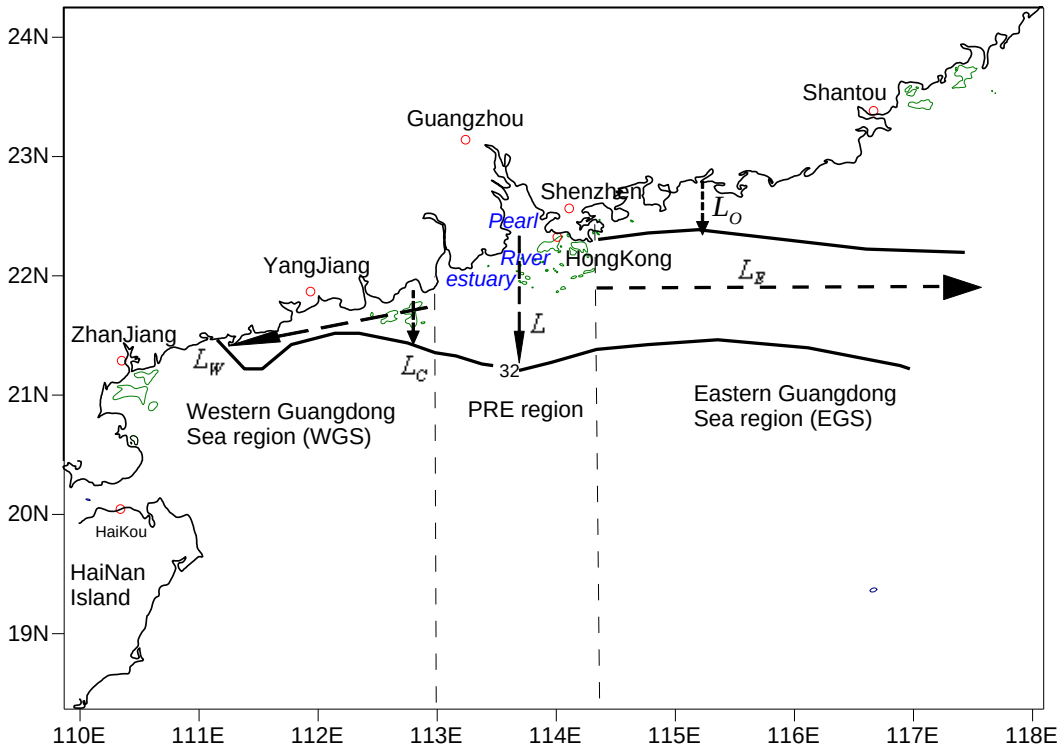

Figure 3: The classification of sea regions, and the definition of plume parameters.

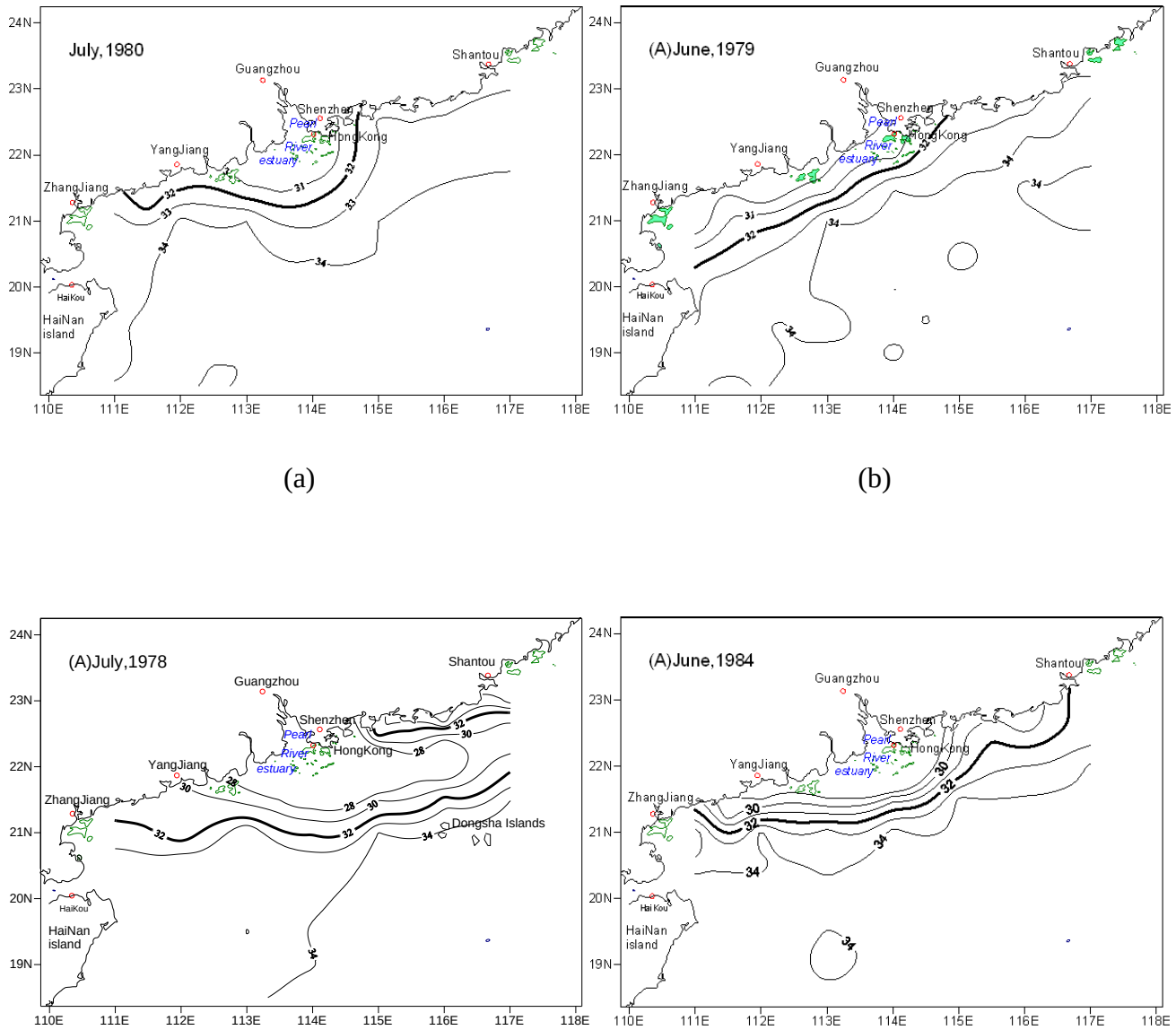

(a) (b)

(c) (d)

Figure 4: (a) Type I - Offshore Bulge Spreading in July 1980. (b) Type II - West alongshore spreading in June 1979. (c) Type III - East offshore spreading in July 1978. (d) Type IV - Symmetrical alongshore spreading in: June 1984,

(a) Vertical salinity profile of Type Ⅰ
across 113° E ,July 1980

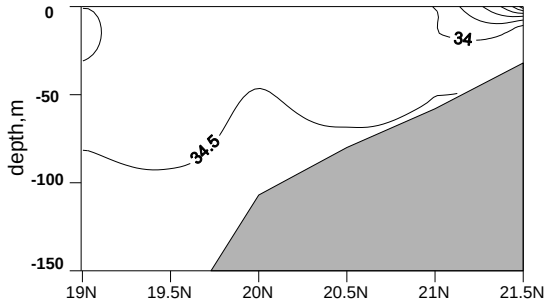

(d) Vertical salinity profile of Type Ⅱ
across 113° E ,June 1979

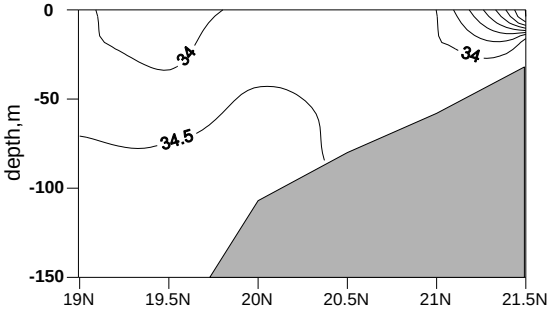

(b) Vertical salinity profile of Type Ⅰ
across 114° E ,July 1980

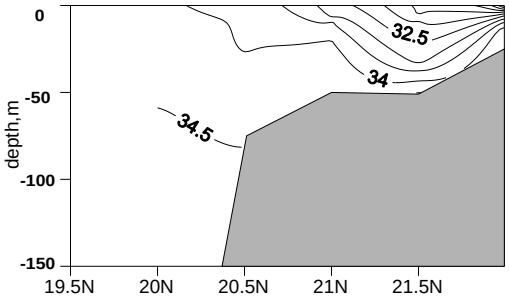

(e) Vertical salinity profile of Type Ⅱ
across 114° E ,June 1979

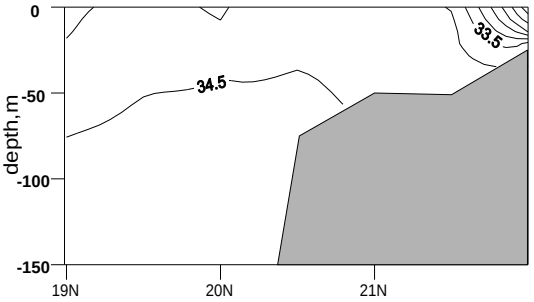

(c) Vertical salinity profile of Type Ⅰ
across 115° E ,July 1980

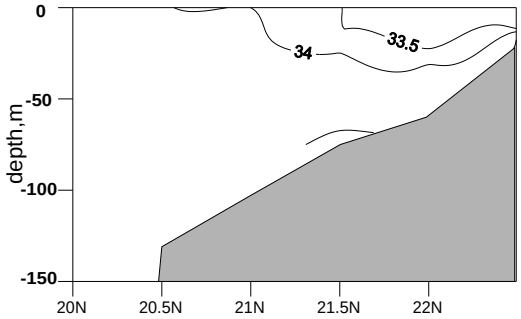

(f) Vertical salinity profile of Type Ⅱ
across 115° E ,June 1979

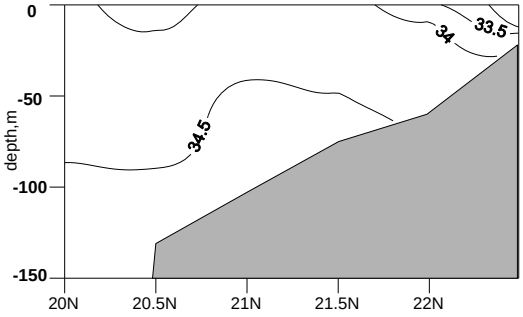

1

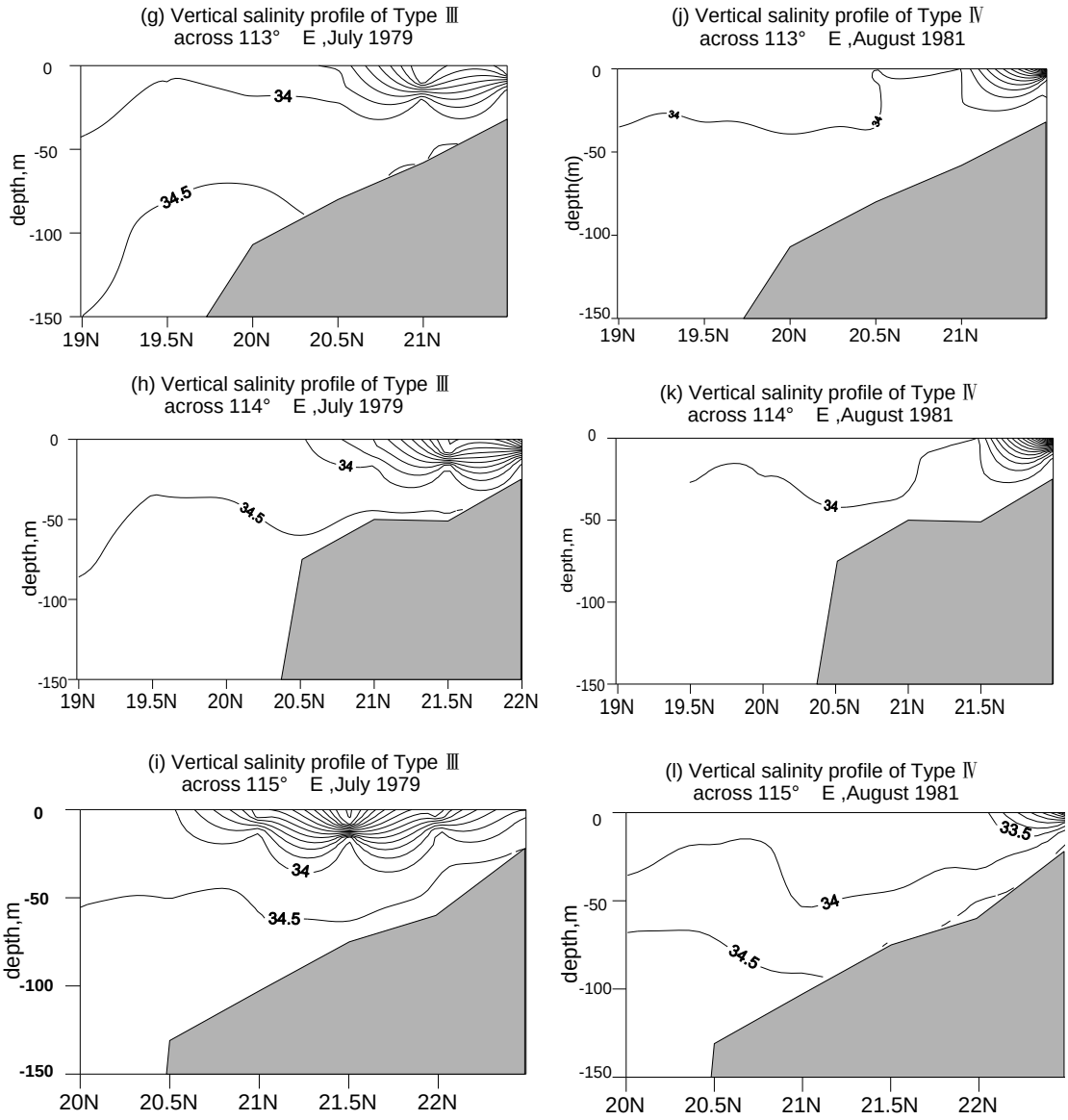

Figure 5: Vertical profiles of the salinity distribution, in which, (a)-(c) are Type I plumes, (d)-(f) are Type II plumes, (g)-(i) are Type III plume, (j)-(l) is Type Ⅳ plume. The salinity contour interval is *0.5 psu*.

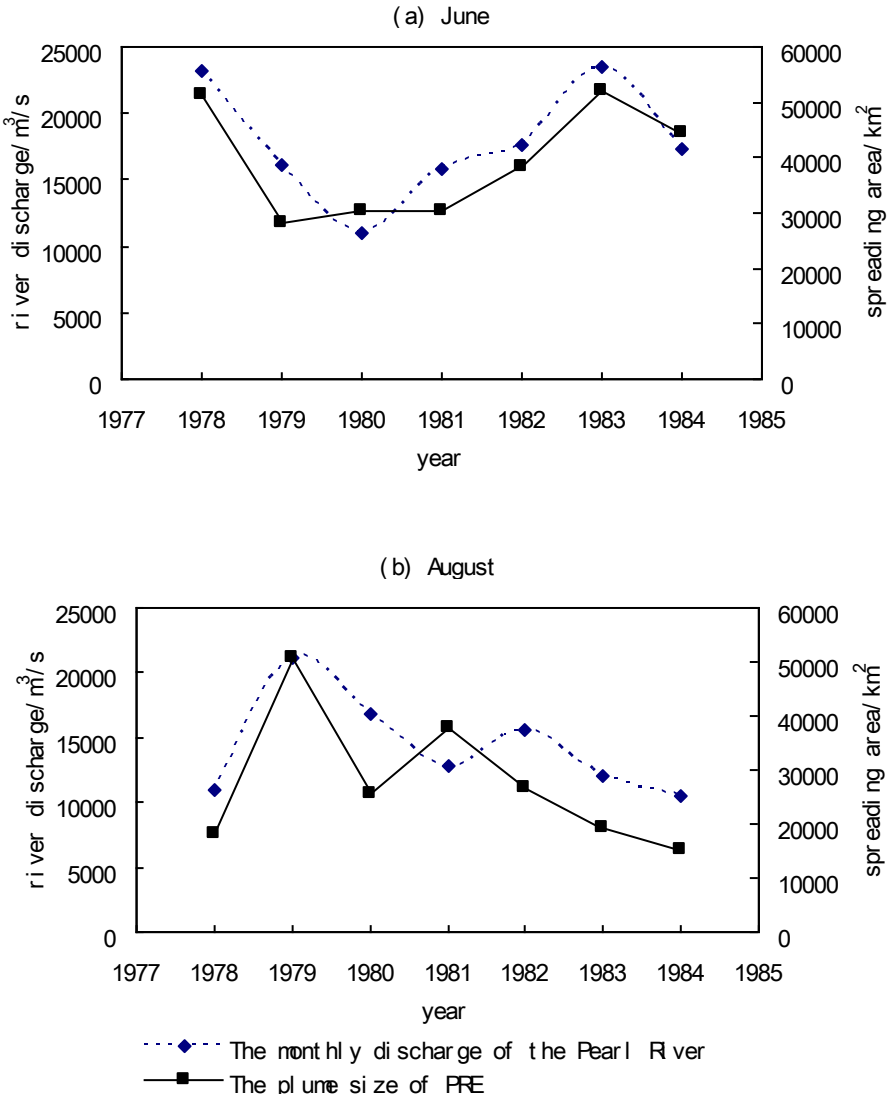

Figure 6: The variations of the spreading area of the PRE buoyant plume and the Pear River discharge in June and August.

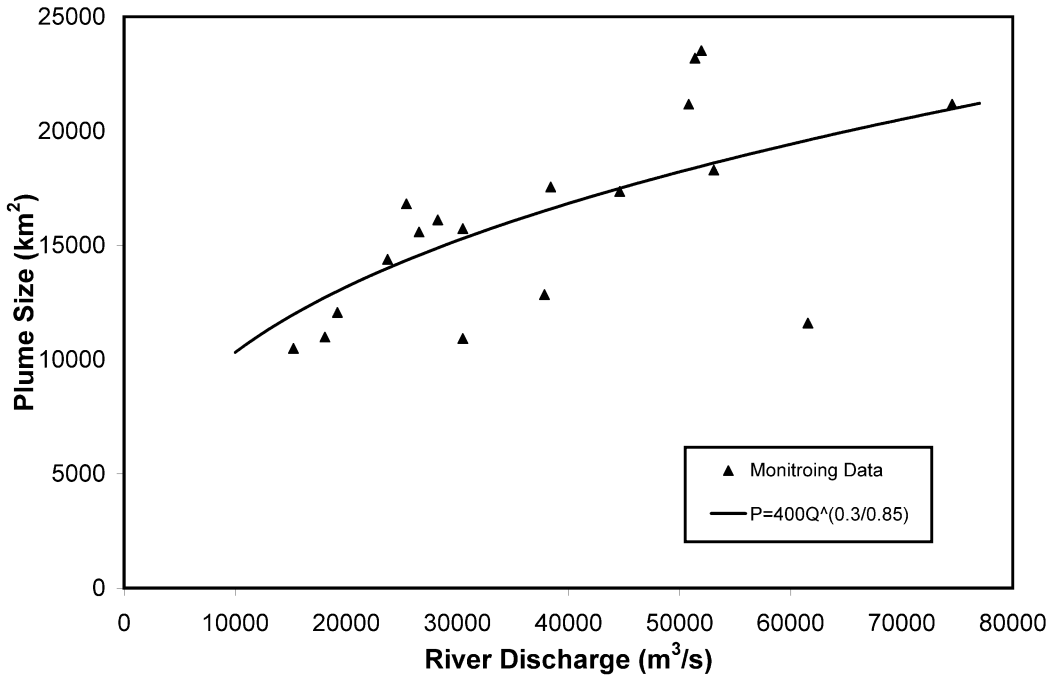

1

2 Figure 7: The relationship between the river discharge and the plume size.

3

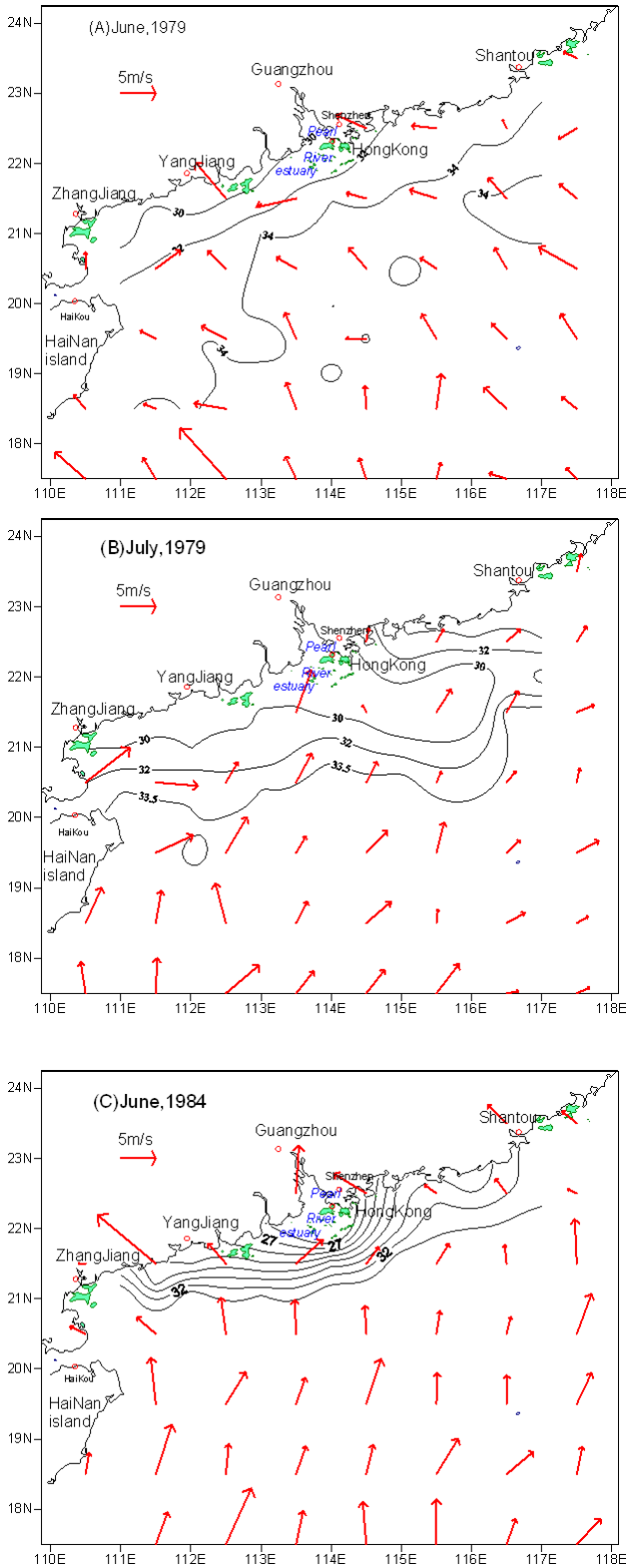

Figure 8: Monthly averaged wind fields (vectors), and the distributions of surface salinity, (A) in June 1979, (B) in July 1979, and (C) in June 1984.

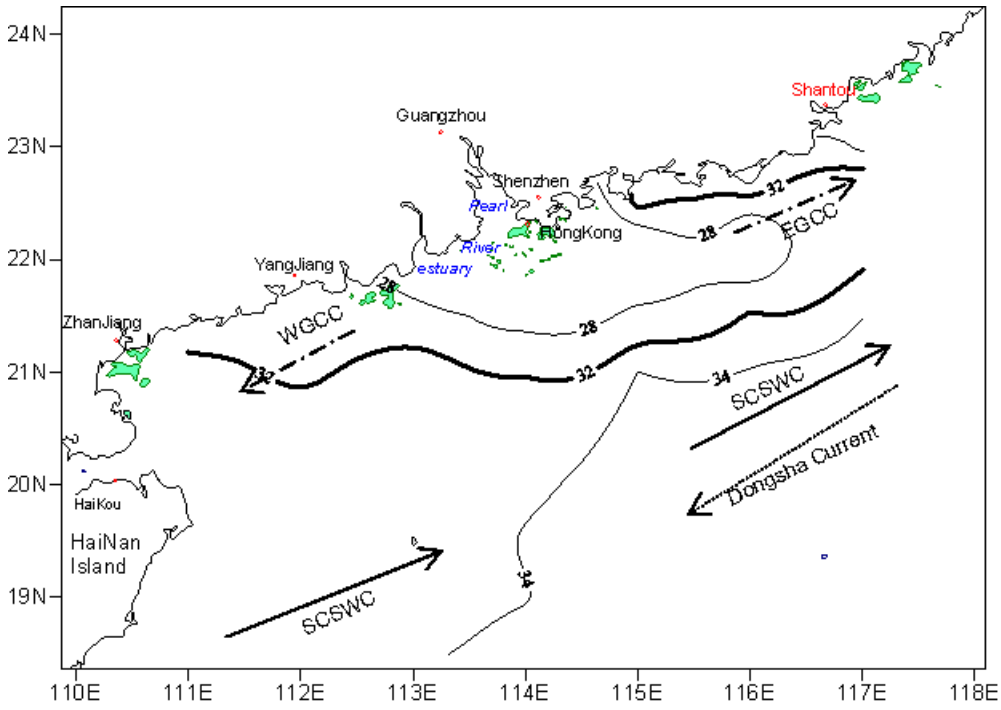

Figure 9: Circulations on the northern of SCS during summer, where EGCC is the Easterly Guangdong Coastal Current, WGCC is the Westerly Guangdong Coastal Current, the isobath is the distribution of surface salinity in July 1978.

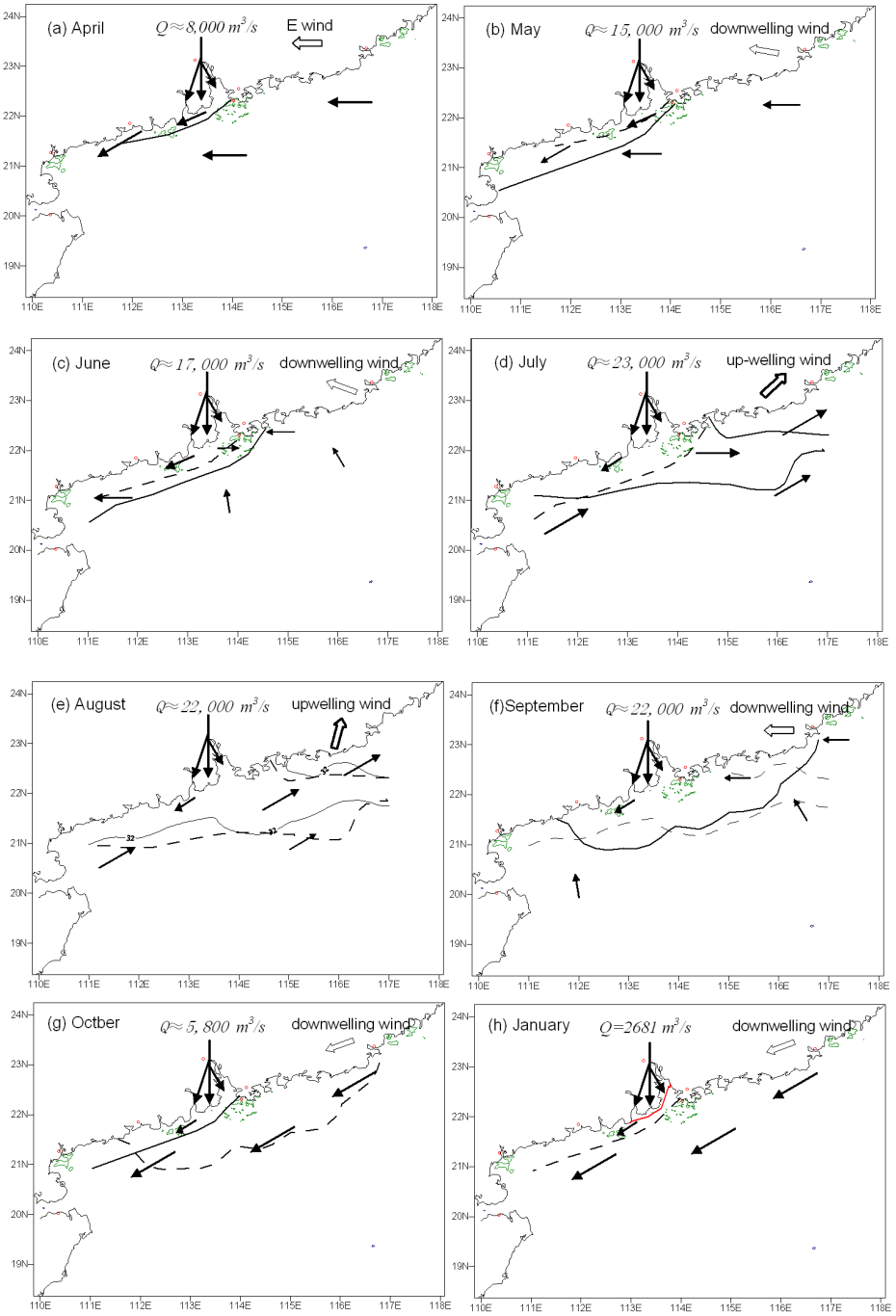

Figure 10: The evolution of the PRE plume. (The solid line represents the *32 psu* isohaline and the dashed line represents the plume boundary of previous month.)

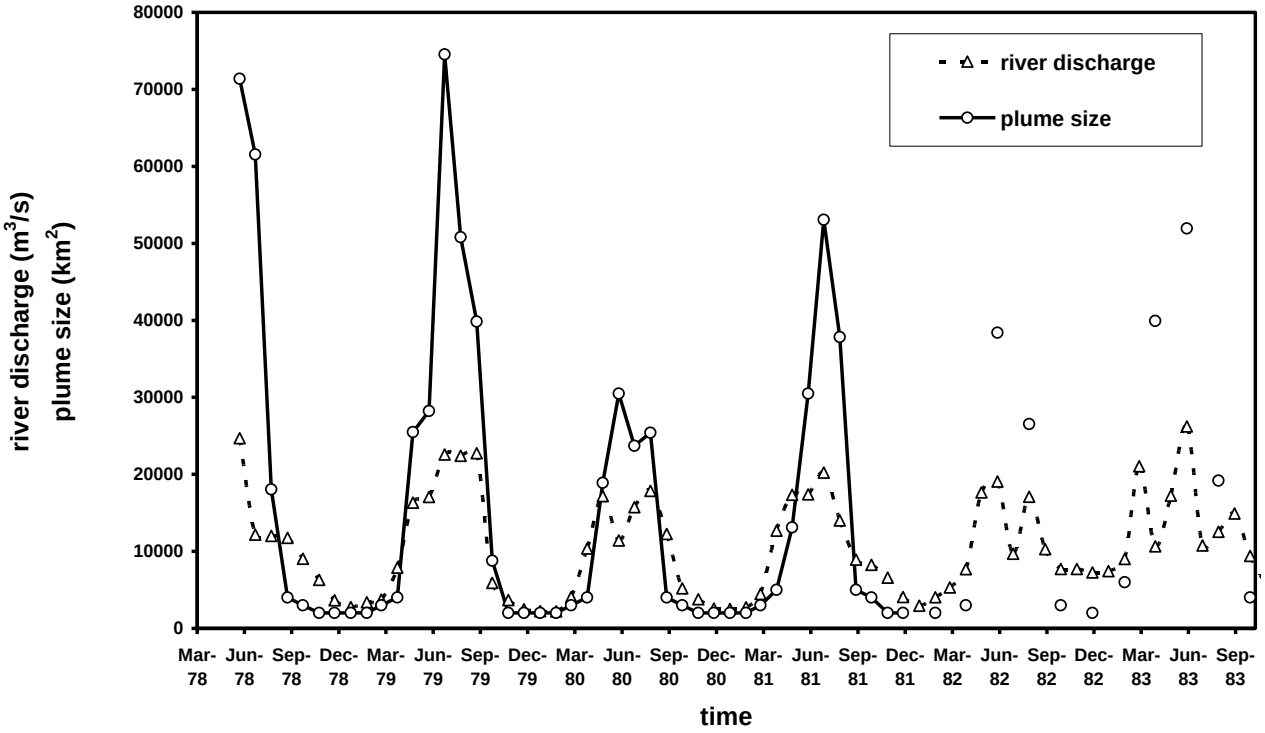

1

2 Figure 11: The monthly variations of plume size and the corresponding river discharge during 1978 to

3 1983.

4

Table 1: The dominant wind and its frequency in the northern shelf of SCS (Ma et al., 1990)

Location		Jan.	Feb.	Mar.	Apr.	May	Jun.	Jul.	Aug.	Sep.	Oct.	Nov.	Dec.
EGS	Dominant wind	NE	NE	NE	E	NE	E	SW	SW	NE	NE	NE	NE
	Frequency (%)	61	54	27	21	17	26	48	30	61	61	83	72
PRE	Dominant wind	NE	NE	E	E	S	S	SW	E	E	NE	NE	NE
	Frequency (%)	59	45	34	32	27	27	33	31	44	42	60	47
WGS	Dominant wind	NE	NE	E	E	E	S	SE	S	E	NE	E	NE
	Frequency (%)	50	52	50	29	41	37	47	23	46	35	50	57

1

2 Table 2: Characteristic parameters of the buoyant plume off PRE in summer.

Time	Plume size km^2	L km	L_E km	L_W Km	L_C km	L_O km	λ	λ_1	Plume type
Jun. 1978	51386	155	102	332	176.0	0	0.9	0.7	II
Jun. 1979	28234	66	51	184	110.0	0	0.6	0.3	II
Jun. 1980	30493	122	102	133	90.0	0	1.4	0.8	II
Jun. 1981	30493	22	0	245	132.0	0	0.2	0.0	II
Jun. 1982	38398	111	102	184	88.0	0	1.3	0.6	II
Jun. 1983	51951	133	296	56	110.0	0	1.2	5.3	IV
Jun. 1984	44610	122	286	128	80.0	0	1.5	2.2	IV
Jul. 1978	61550	161	286	133	143.0	110	1.1	2.2	III
Jul. 1979	74538	149	286	245	176.0	103	0.8	1.2	III
Jul. 1980	23717	116	31	56	33.0	0	3.5	0.6	I
Jul. 1981	53080	122	275	82	132.0	35	0.9	3.4	III
Aug. 1978	18070	33	0	112	93.5	0	0.4	0.0	II
Aug. 1979	50821	122	296	102	132.0	110	0.9	2.9	III
Aug. 1980	25411	89	214	5	99.0	63	0.9	42.8	III
Aug. 1981	37834	133	296	92	93.5	0	1.4	3.2	IV
Aug. 1982	26540	55	194	87	88.0	0	0.6	2.2	IV
Aug. 1983	19199	55	41	107	71.5	0	0.8	0.4	II
Aug. 1984	15246	89	41	41	44.0	0	2.0	1.0	I

3

Table 3: The relationship between the buoyant plume type and the wind strength index.

Time	W_{dir} Wind direction	U_{10} (m/s) Wind Speed	I_w Wind Strength Index	Plume type
Jun. 1978	E, ESE	2.6	1.96	II
Jun. 1979	E, ESE	3.2	1.79	II
Jun. 1980	E, SE	3.3	1.91	II
Jun. 1981	E	2	1.45	II
Jun. 1982	E	1.5	1.63	II
Jun. 1983	S~SE	3.4	-1.14	IV
Jun. 1984	S, SW	3.5	1.05	IV
Jul. 1978	SW, SWW	2.2	-1.81	III
Jul. 1979	SW, SWW	3.3	-2.99	III
Jul. 1980	S, SSE	2.3	0.45	I
Jul. 1981	SSW, SSE	4.1	-2.45	III
Aug. 1978	E	2.6	1.43	II
Aug. 1979	SSW, SW	2.6	-1.95	III
Aug. 1980	SSW	3.8	-2.01	III
Aug. 1981	SW, SWW	2.1	-1.16	IV
Aug. 1982	S, SSW	2.8	-1.51	IV
Aug. 1983	S, SE	2.1	1.43	II
Aug. 1984	S	1.7	-0.69	I

Table 4: The governing parameters and plume characteristics summarized for the four types of horizontal buoyant plumes.

	Type Ⅰ	**Type Ⅱ**	**Type Ⅲ**	**Type Ⅳ**
λ_I	≈ 1	<1	>1	>1
L_O	0	0	>0	0
λ	>1.7	<1.7	<1.7	<1.7
plume size	relative small	varied	relative large	large
river discharge	small	varied	large	varied
wind	weak up-welling wind	down-welling wind	strong up-welling wind	varied wind directions

Dr Hong Zhang

Griffith School of Engineering
Gold Coast Campus, Griffith University
PMB 50 Gold Coast MC
Queensland 9726
Australia

Telephone +61 (0)7 5552 9015
Facsimile +61 (0)7 5552 8065
Email hong.zhang@griffith.edu.au

July 29, 2009

Prof Benoit Cushman-Roisin
Editor-in-Chief, Environmental Fluid Mechanics

Dear Prof Cushman-Roisin,

Thank you and reviewers for your review reports on the article of "Dynamics of the Buoyant plume off the Pearl River Estuary in summer" (Ref: EFMC219). We have completed the minor revision according to the reviewers' second comments. Shown below are the details of my responses to the reviewers' comments.

Reviewer #1:

1. Table 3 is not available with the pdf file provided for review. If it indeed contains the information as indicated in the caption and the main text, it will be very useful to the readers.
   Table 3 was included. It might be PDF generation error that the reviewer couldn't see it. I checked the revised version that Table 3 was presented.

2. A table summarized the governing parameters and plume characteristics for the four types of horizontal buoyant plumes.
   A new Table 4 has been added in Page 34 as suggested which has been referred in Conclusion.

3. In the abstract, a definitive concluding statement should be added.
   Abstract has been revised.

4. In Figure 5g), h) & i) , can the authors explain why there are multiple points where large vertical gradient (contour lines attracted together) occurred along the plume? Are they related to the availability of measured data?
   Yes, this is due to the limited availability of measured data (the vertical profiling distance is between *5 m* to*10 m*).

5. The authors still used the word "bugle" instead of "bulge" in a couple of places in the manuscript.
   Corrected.

6. In line 18, it will be better to add "two" between "last decades".
   Corrected.

Reviewer #2:

First, I apologize to the authors for my slow review. I have had some extenuating circumstances at home during the spring.

I think that the authors have made some substantial improvements to their manuscript, especially with respect to the more quantitative description of the wind's influence. Their data are a nice validation of the Whitney and Garvine scaling. They have also added an interesting section on plume evolution. Although the manuscript has been improved, I still think that some significant further improvements are necessary to meet the potential of this interesting data set and the expectations for the journal.

As it is written, the manuscript primarily documents the agreement between the observations and previously established plume theory: larger discharge leads to larger plume (Walker, 1996; Warrick and Fong, 2004) and up- / down-welling winds shift the plume up- / down-shelf (many; Whitney and Garvine, 2005). While there is value in this comparison, not a lot that is new has been learned about plumes. The authors touch on some interesting conclusions on page 15 relating to the timing of the plume evolution:

"The buoyant plume characteristics in summer also varies. It depends on the starting time of the wet season, the flood intensity and when the summer monsoon breaks out. If the wet season begins early, such as in 1983 when the wet season begins in March and the largest river discharge occurs in May, 16 Type III plume is formed in May and then Type IV plume exists in June."

However, this line of reasoning is not really proven or clearly demonstrated in the paper. In my first review I suggested that the authors consider the lag time in plume evolution. The timescales of wind adjustment are too short to be captured with the current data set, but the lag between discharge and plume area may be captured. Some of this information can be inferred from Figure 6, but I believe that this could be presented more clearly as monthly time series over the whole year. Would it be possible to plot the plume area for each month of the year so that it can be compared directly with the monthly discharge data in Fig 2 (thank you for adding that)? It may be informative to see if there is a consistent lag between Q and plume area and determine an average across the study years. Comparison of the lag in different years may also lead to insights about how the wind conditions in a given year modify the discharge - area relationship. Many of these ideas are already discussed in the text, but they are not analyzed or quantified. Any lag in the discharge area relationship is largely ignored in previous work. This is a possible new contribution from the current work if it proves fruitful.

A new Figure 11 (The monthly variations of plume size and the corresponding river discharge) has been added to show the lag between the river discharge and the plume area. The lag is small in normal conditions. But the figure helps to explain the plume evolution better. Figure 11 has been discussed in Page 14.

My concerns about the first submission by Ou et al were that it needed: 1) a more quantitative analysis of the forcing of the plume, 2) better integration of current literature that relates to plume dynamics and 3)the focus could be changed a bit to make this study relevant to plumes other than the PRE plume.

Below I comment on the changes made to address these concerns.
1) Quantitative analysis.
The authors have made good use of the wind index. It appears that the classification of the plume behavior agrees very well with Iw. It would be nice to see this comparison graphically instead of in a table.
I still think Table is a better format to present the results, as I_w is an index.

The requested discussion of the Rossby number in section 4.1 is cursory and does not add anything to the manuscript. It should be expanded on or cut.
Removed as suggested.

2) Previous literature:
The suggested previous literature has been mentioned.

3) Focus
While the authors appear to have covered the relevant literature in their introduction, it is still structured primarily as a list rather than an informative discussion. For example, instead of "A conceptual model was developed to study the impact of an upwelling wind to the surface-advected plume by Fong and Geyer (2001)," it would be valuable to the reader if the main conclusion(s) of the Fong and Geyer paper

relevant to the present work was summarized. This would lead to a better summary of what remains to be learned about plumes.

Other comments:
The paper (still) needs to be read thoroughly for language, grammar and style. I have only noted a few errors of that type in the following.
Pg 5 - change transactions to transects.
Pg 8. The citation for eq 2 and 3 both appear to be Horner-Devine et al, but at least 2 and perhaps 3 should really be Yankovsky and Chapman. I think that is intended, but the wording needs to be improved.
Pg 10 Hichey should be changed to Hickey.
Pg 10 "Surface winds drive the surface water flowing and the buoyant plume moving." Needs to be re-written.
Pg 11 "Tpye II plume".
Pg 12 line 6, State where these velocity ranges come from.
Conclusions: Too many nested lists. Write as paragraphs.
Abstract, Introduction and Conclusion have been revised accordingly. All above minor changes have also been completed.

I would also like to thank you and the reviewers for your valuable comments, which have significantly improved the quality of this paper.

Yours sincerely,

Hong Zhang